How to cite: *Angew. Chem. Int. Ed.* **2022,** *61,* e202201573
International Edition: doi.org/10.1002/anie.202201573
German Edition: doi.org/10.1002/ange.202201573

Systems Chemistry | Hot Paper

Self-Regulating Colloidal Co-Assemblies That Accelerate Their Own Destruction via Chemo-Structural Feedback

*Charu Sharma and Andreas Walther**

Abstract: Biological self-assemblies self- and cross-regulate each other via chemical reaction networks (CRNs) and feedback. Although artificial transient self-assemblies have been realized via activation/deactivation CRNs, the transient structures themselves do mostly not engage in the CRN. We introduce a rational design approach for chemo-structural feedback, and present a transient colloidal co-assembly system, where the formed co-assemblies accelerate their destruction autonomously. We achieve this by immobilizing enzymes of a deactivating acid-producing enzymatic cascade on pH-switchable microgels that can form co-assemblies at high pH. Since the enzyme partners are immobilized on individual microgels, the co-assembled state brings them close enough for enhanced acid generation. The amplified deactivator production (acid) leads to an almost two-fold reduction in the lifetime of the transiently formed pH-state. Our study thus introduces versatile mechanisms for chemo-structural feedback.

Biological systems have the capability to assemble relatively simple building blocks into ordered yet dynamic structures that self-regulate and cross-regulate each other autonomously via complex networks of chemical reactions, feedback loops, and/or energy dissipation. This gives rise to emergent properties like signal-processing, motion, and adaptation.[1] In contrast, in synthetic systems, there have been significant advances in hierarchical self-assemblies (SAs) and in making those switchable by sequential application of external "on"/"off" triggers (e.g., pH).[2] However, such systems do typically not feature higher levels of autonomous behavior or self-regulation. Autonomous dynamics and self-regulatory control require the antagonistic pathways of reversible SAs to be pre-organized using appropriately designed kinetics in networks of antagonistic (activating/deactivating) reactions.[1c,3] This generates a time-lapse between activation and deactivation necessary for controlling the time-domain of SAs. Most successful approaches to realize SAs with programmable lifecycles involve either so-called dissipative environments to which a SA is coupled, that is for instance pH-feedback curves,[4] or enzymatic ATP-degradation in ATP-co-assembling systems,[5] or so-called dissipative structures, whereby a building block is temporally activated for SA using a chemical fuel.[6]

However, in most of these approaches towards temporally programmed, non-equilibrium systems, the intermediately formed SA does not distinctly participate in the deactivation pathways. This is, in fact, unlike biological structures, e.g., microtubules, that feature a catalytic pocket for GTP hydrolysis that activates for GTP hydrolysis when the assembly is formed.[7] Such a mechanism—a chemo-structural feedback process—would extend beyond principles of pure chemical feedback and allow for new types of self-regulatory behavior and cooperativity. Only a handful of examples exist—most notably from the peptide and nanofiber SA field—in which dissipative structures engage in the reaction network to catalyze downstream processes.[8] However, rational design of building blocks in such systems remains a challenging task.

To address the challenge of designing chemo-structural feedback, we introduce a concept for temporally self-regulating co-assembling microgel (MG) systems, whereby the assembly of the MGs accelerates its own disassembly. The concept makes use of a pre-organized pH-feedback system (pH-FS), wherein an alkaline trigger leads to assembly, while the counter-trigger is provided by an acid-producing enzymatic cascade (EC). Critically, the two components of the EC are immobilized on individual MGs such that the transient MG co-assembly brings them close enough to enhance the production of the acidic deactivator. The system thereby features an amplified deactivator generation, demonstrating advanced chemo-structural feedback; namely, co-assemblies promote their own destruction.

In more detail, the key concept relies on coupling elements of a deactivating, acid-producing EC (invertase/glucose oxidase; INV/GOX) to pH-switchable, co-assembling MGs (Figure 1a). We chose MGs because they are well dispersible, can be surface-functionalized with interact-

[*] C. Sharma, Prof. Dr. A. Walther
A3BMS Lab, Department of Chemistry
University of Mainz
55128 Mainz (Germany)
E-mail: andreas.walther@uni-mainz.de
Prof. Dr. A. Walther
Cluster of Excellence livMats @ FIT
Freiburg Center for Interactive Materials and Bioinspired Technologies
University of Freiburg
79098 Freiburg (Germany)

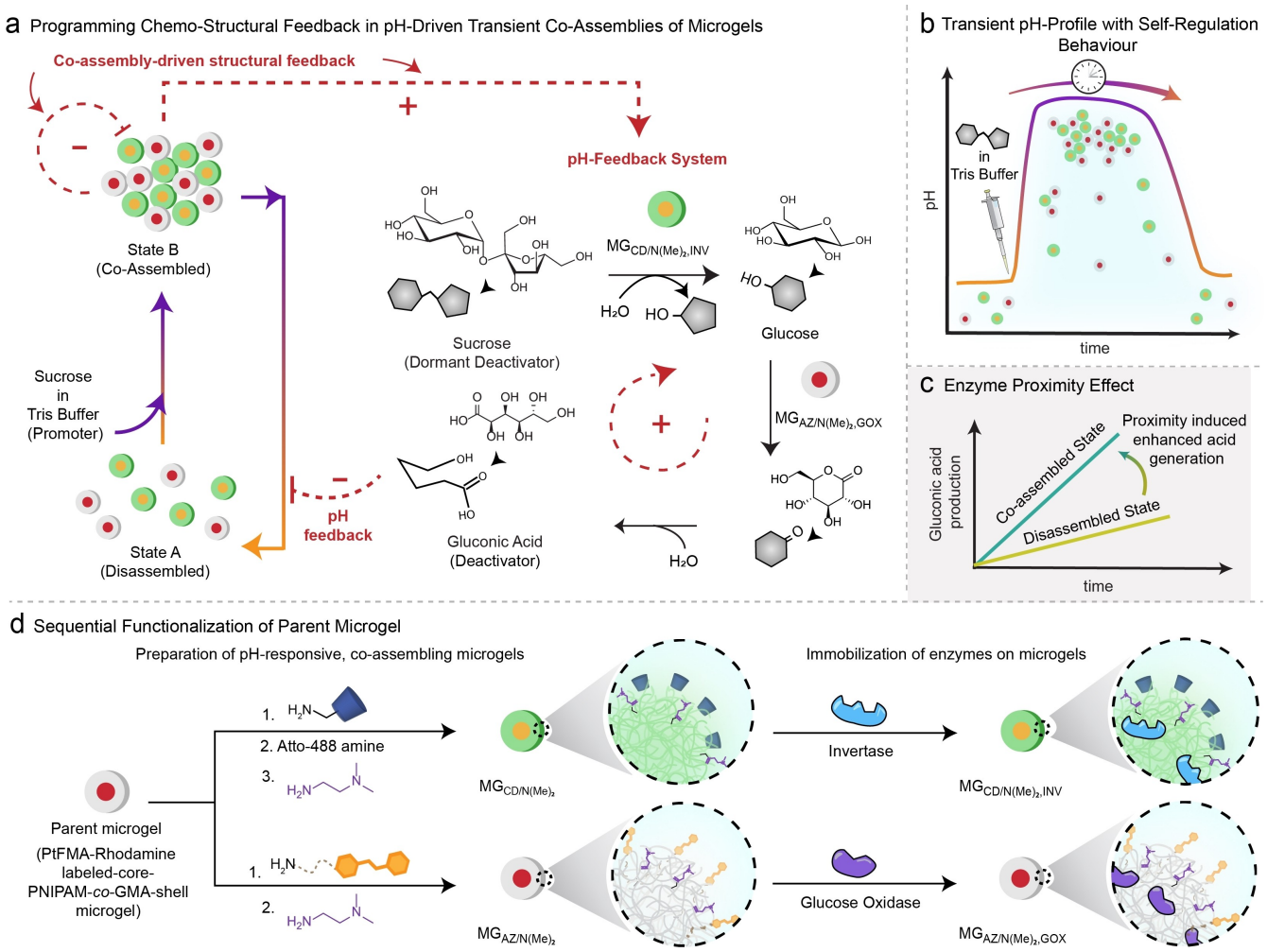

Figure 1. System design for rational design of chemo-structural feedback in pH-driven transient co-assemblies of MGs. a) Addition of promoter (tris buffer) triggers the transient co-assembly of two pH-responsive MGs, b) whereby each MG carries one enzyme partner of the acid-producing EC (Invertase/Glucose Oxidase; INV/GOX). The EC converts sucrose (dormant deactivator) to gluconic acid which drives the system back to the disassembled state (State A) hence providing negative feedback to the co-assembled state (State B). c) Enzyme proximity in State B provides a chemo-structural feedback, leading to strongly amplified acid generation and faster disassembly. d) Sequential functionalization of parent MGs generate two pH-responsive and co-assembling MGs ($MG_{CD/N(Me)2}$ and $MG_{AZ/N(Me)2}$) followed by successive enzyme immobilization ($MG_{CD/N(Me)2,INV}$ and $MG_{AZ/N(Me)2,GOX}$).

ing groups, and most importantly, can harbor functional molecules (i.e., enzymes) in their interior to allow implementing features of an embodied intelligence for autonomous operation.[9] The MGs need to be equipped with adhesive hetero-complementary supramolecular units (α-cyclodextrin = CD, and azobenzene = AZ) to allow for ordered co-assembly, as well as with weak cationic groups ($-N(Me)_2$) to allow for assembly at high pH and repulsive behavior at low pH. Additionally, each MG partner needs to be equipped with one enzyme of the EC (Figure 1d).

In a final system, starting from a ground State A, where both MGs ($MG_{CD/N(Me)2,INV}$ and $MG_{AZ/N(Me)2,GOX}$) are well dispersed in citric acid/sodium citrate buffer (CA/Na_3C), a solution of an alkaline promoter (tris buffer) containing sucrose as chemical fuel (dormant deactivator) is added. The tris buffer lifts the system to State B thereby activating the MG co-assembly (Figure 1b). Concurrently, $MG_{CD/N(Me)2,INV}$ catalyzes the hydrolysis of sucrose to the intermediates glucose and fructose. As a result of the co-assembly, the glucose only has a short diffusive pathway to the GOX on $MG_{AZ/N(Me)2,GOX}$ to yield gluconic acid δ-lactone and finally gluconic acid (Figure 1 b,c, Figure S1). The latter serves as a deactivator and induces disassembly.

We employed MGs with core–shell architecture.[2c,d,9a,10] The MGs are composed of a water-insoluble poly(2,2,2-trifluoroethyl methacrylate) (PtFMA) core that is refractive index-matched with water and labeled with Rhodamine B for Confocal Fluorescence Laser Scanning Microscopy (CLSM). These cores are surrounded by a water-soluble hydrogel shell composed of *N*-isopropylacrylamide (NIPAM, 90 wt%), *N*,*N*′-methylenebis(acrylamide) (MBA, 1 wt %), and glycidyl methacrylate (GMA, 9 wt%) (Figure 2a, Supporting Information 4.1 and 4.2). The MGs have a *z*-average radius, $<R_h>_z$, of 649 nm with a core of $<R_h>_z =$

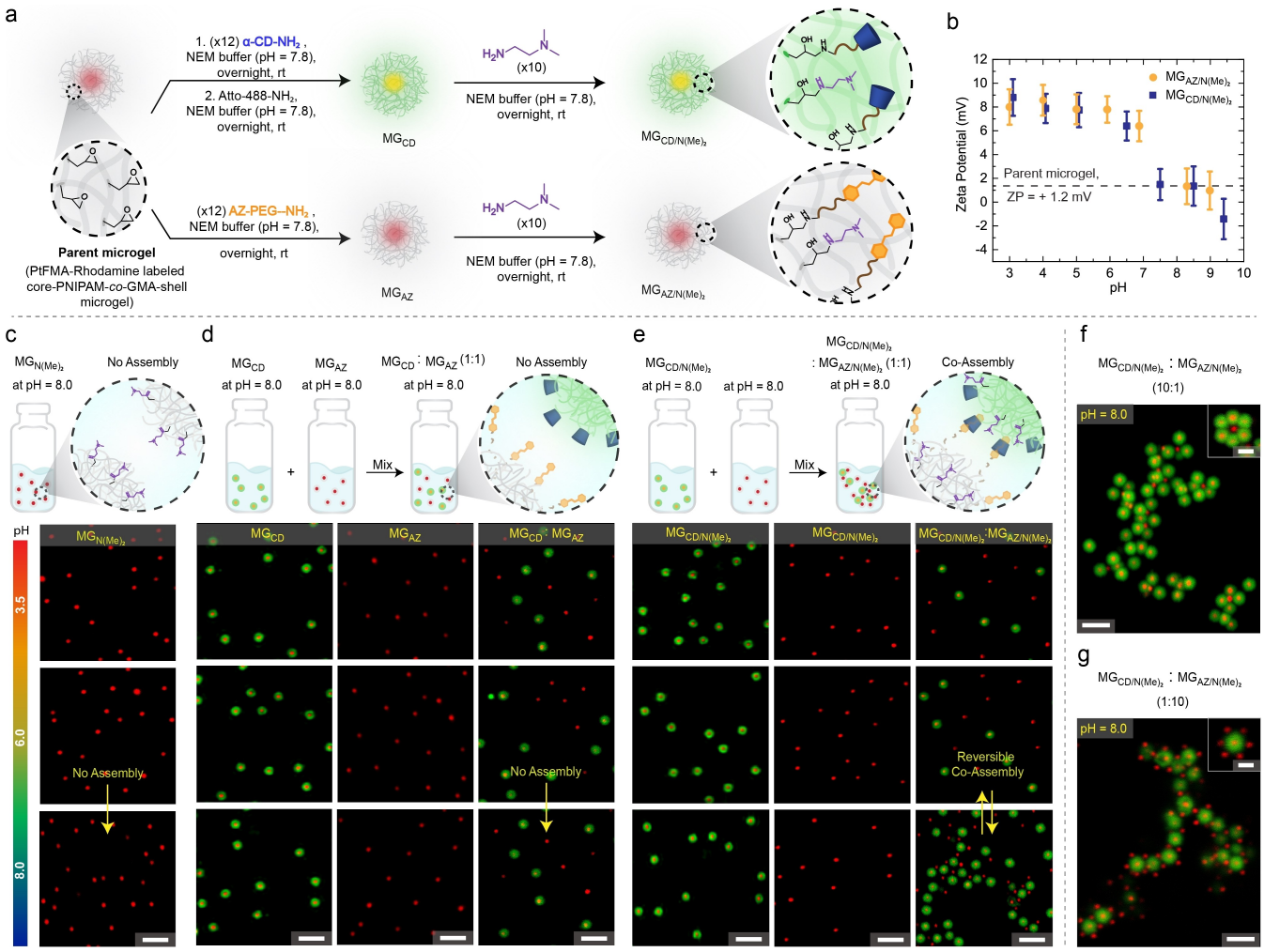

Figure 2. Synthesis and characterization of two co-assembling MGs. a) Synthesis scheme for $MG_{CD/N(Me)2}$ and $MG_{AZ/N(Me)2}$ (Supporting Information 4.4). Rhodamine B labels (red channel) are present in the core, while only the shells of CD-containing MGs are labelled with Atto-488 (green channel) to differentiate them from $MG_{AZ/N(Me)2}$. b) pH-dependent zeta-potential of $MG_{AZ/N(Me)2}$ and $MG_{CD/N(Me)2}$. Error bars represents the standard deviation from three independent measurements. c, d) pH-dependent CLSM images of $MG_{N(Me)2}$, MG_{CD}, MG_{AZ} and 1:1 mixture of MG_{CD} and MG_{AZ}. e) pH-dependent CLSM images of $MG_{CD/N(Me)2}$, $MG_{AZ/N(Me)2}$ and 1:1 mixture of $MG_{CD/N(Me)2}$ and $MG_{AZ/N(Me)2}$. Co-assemblies only occur for the desired $MG_{AZ/N(Me)2}$/$MG_{CD/N(Me)2}$ mixture at pH 8.0 and disassemble reversibly at acidic pH. Scale bars (c–e), 3 μm. f, g) Hierarchical structures for non-stoichiometric mixtures of $MG_{CD/N(Me)2}$ and $MG_{AZ/N(Me)2}$. Scale bars: f, g) 3 μm; scale bars in insets: 1 μm. The final concentration of MGs in all suspensions is 0.0064 wt%.

198 nm as measured by dynamic light scattering (DLS) at pH 7 (Figure S2).

The initiator (2,2′-azobis(2-methylpropionamidine) dihydrochloride) used for the synthesis imparts a minimal positive charge (zeta (ζ)-potential value = +1.2 mV) to the MGs, that is constant across the entire pH range (Figure 2b).

To integrate the MG system to a pH-FS in an alkaline regime (Figure 1a), the prospective building blocks must be capable of forming reversible SAs at alkaline pH (pH 8–9). Additionally, a hetero-particle aggregation with controlled co-assembly is beneficial to assure spatial proximity of the enzymes of the EC in the co-assembled state. To meet these requirements, we co-functionalized the MGs with pH-responsive *N,N*-dimethylethylenediamine (DMEDA, pK_a ≈10.2) and the CD/AZ pairs.[2c,d,11] CD and AZ are immobilized separately on two batches.

This leads to $MG_{AZ/N(Me)2}$ and $MG_{CD/N(Me)2}$ (Figure 2a, synthetic details in Supporting Information 4.4, Figure S3). Additionally, we synthesized control MGs, bearing only the DMEDA groups ($MG_{N(Me)2}$) or only the CD and AZ groups (MG_{CD} and MG_{AZ}) using the same reaction protocols to maintain a close to identical functionalization, respectively.[12]

pH-dependent ζ-potential measurements of the amine-modified MGs ($MG_{AZ/N(Me)2}$ and $MG_{CD/N(Me)2}$, $MG_{N(Me)2}$) show a continuously increasing electrostatic repulsion when reducing the pH from 9 to 3 due to increased protonation of the $N(Me)_2$ groups (Figure 2b, Figure S4). This contrasts the constant ζ-potential for the parent MGs (flat line in Figure 2b). For accurate treatment of ζ-potential measure-

ments, that are not hard sphere colloids, we refer to literature by Saunders and group.[13] The successful functionalization is further corroborated by DLS, which, for instance, shows a size increment of ≈70 nm in the case of MG_{AZ} to $MG_{AZ/N(Me)2}$ functionalization due to increased repulsion between the protonated $N(Me)_2$ groups (Figure S2).

To probe for the selective co-assembly at alkaline pH, we visualized the dispersions of the controls and of the relevant mixtures via CLSM at pH 3.5, 6.0 and 8.0 (Figure 2c,d). For better visualization, the MGs bearing CDs were labeled with a green-emitting dye (Atto-488, Supporting Information 4.4.3), while only the cores are visible in red for the other MGs. Gratifyingly, only mixtures of $MG_{AZ/N(Me)2}$ and $MG_{CD/N(Me)2}$ assemble at high pH, and they do so reversibly (Figure 2e, Figure S6). The control, $MG_{N(Me)2}$, does not assemble at high pH (Figure 2c). This underscores that the low ζ-potential and the slightly hydrophobic stickiness of the deprotonated $N(Me)_2$ groups alone are insufficient for assembly at high pH, but that the attractive interactions provided by the CD/AZ pair are important for the co-assembly. Similarly, the mixture of MG_{AZ} and MG_{CD} without $N(Me)_2$ does also not assemble at high pH, which we associate to the lack of some beneficial hydrophobicity effect of the deprotonated $N(Me)_2$ groups in the co-functionalized MG system (Figure 2d). Hence both components are important to jointly promote co-assembly at high pH. Non-stochiometric ratios of $MG_{CD/N(Me)2}$ and $MG_{AZ/N(Me)2}$ lead to core-satellite structures, which underscores that co-assemblies are primarily based on hetero-complementary recognition units, assisted by some hydrophobic effects from $N(Me)_2$ (Figure 2 f,g). Overall, these building blocks and their behavior are the first steps towards chemo-structural feedback.

To integrate these pH-switchable building blocks with a self-regulating feature brought about by the EC, the MG offsprings bearing the supramolecular units need to be functionalized with the individual enzymes. To this end, CD-functionalized MGs (MG_{CD} and $MG_{CD/N(Me)2}$) were coupled with INV (Figure 3a, Supporting Information 4.5.1) and AZ-modified MGs (MG_{AZ} and $MG_{AZ/N(Me)2}$) with GOX (Figure 3b, Supporting Information 4.5.2). Since immobilization can change enzyme activities,[14] we characterized the respective activities using fluorometric activity assays (details on the activity assays are in Supporting Information 4.6, Figure S5; Figure 3c,d). Both assays probe for the oxidation of a substrate that is generated by the H_2O_2 side product of the GOX-mediated oxidation of glucose. This means that free GOX has to be present in the activity assay for INV-modified MGs to complete the EC. Overall, the activity of immobilized INV on MGs ($MG_{CD,INV,}$ and $MG_{CD/N(Me)2,INV}$) is higher than that of immobilized GOX ($MG_{AZ,GOX,}$ and $MG_{AZ/N(Me)2,GOX}$) (Figure 3c,d). Importantly, for all enzyme-modified MGs, the assays clearly show a substantial catalytic activity required in later stages.

Towards the final system integration, we performed minimalistic pH assays, aiming at the formation of a transient alkaline pH-FS (Figure 3e,f, Supporting Information 4.7). To this end, we injected a mixture of the respective

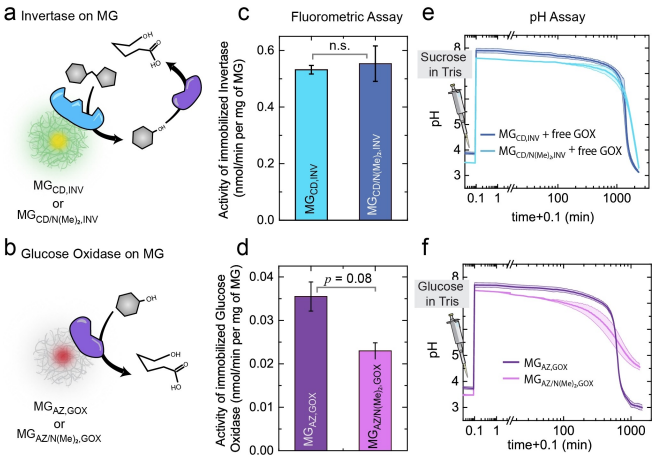

Figure 3. Enzyme immobilization on MGs and their characterization. a, b) Scheme for the catalytic activity. c, d) Quantified activity of covalently immobilized enzymes by fluorometric assay (Supporting Information 4.6). Error bars represent the standard deviation from two independent measurements. *p* value indicated above. n.s. not statistically significant. e, f) Simplified transient pH-curves using only one enzyme-functionalized MG and either sucrose or glucose as fuel, respectively. Free GOX needs to be added in (e) to complete the EC (Supporting Information 4.7). The shaded areas represent the standard deviation from two independent measurements. Conditions: e) 200 mM sucrose, 1.5 mM CA/NA_3C (pH 3.5), 20 mM tris buffer (pH 8.8), 0.14 g L^{-1} GOX (here, we used minimum amount of GOX which is required to complete the EC and furnish transient alkaline pH-FS) and concentration of $MG_{CD,INV}$/$MG_{CD/N(Me)2,INV}$ in the system is 0.0032 wt%.; f) 200 mM glucose, 1.5 mM CA/NA_3C buffer (pH 3.5), 20 mM tris buffer (pH 8.8) and concentration of $MG_{AZ,GOX}$/$MG_{AZ/N(Me)2,GOX}$ in the system is 0.0032 wt%.

fuel (sucrose for INV, glucose for GOX) and tris buffer (20 mM, pH 8.8; promoter) into suspensions containing one of the enzyme-loaded MGs. In the case of the INV systems, GOX is additionally provided in the solution. The starting point is a CA/Na_3CA buffer (1.5 mM, pH = 3.5). In all cases, we find the desired autonomous pH-curves in alkaline regime, which clearly demonstrates the successful operation of the enzymes on the MGs for each individual enzyme-modified MG.

For the final system integration towards co-assembling systems with chemo-structural feedback (CSF), we define two systems: (i) System REF: A reference system incapable of co-assembly using a 1:1 mixture of $MG_{CD,INV,}$ and $MG_{AZ,GOX}$ (Figure 4a). (ii) System CSF: Capable of co-assembly, which is composed of a 1:1 mixture of $MG_{CD/N(Me)2,INV}$ and $MG_{AZ/N(Me)2,GOX}$ (Figure 4b). Due to the elemental composition of the MGs, it is not possible to determine the exact quantity of enzyme. This is why we study the system also with enzyme-loaded, but non-assembling MGs (due to lack of supramolecular interactions → System REF). The suspensions for both systems were prepared by mixing the respective MGs in CA/Na_3CA buffer (pH 3.5, 1.5 mM).

The addition of sucrose with the promoter tris buffer (pH 8.8, 20 mM) increases the pH rapidly to ca. pH ≈ 8.0 in both systems (Figure 4c). However, a striking difference in

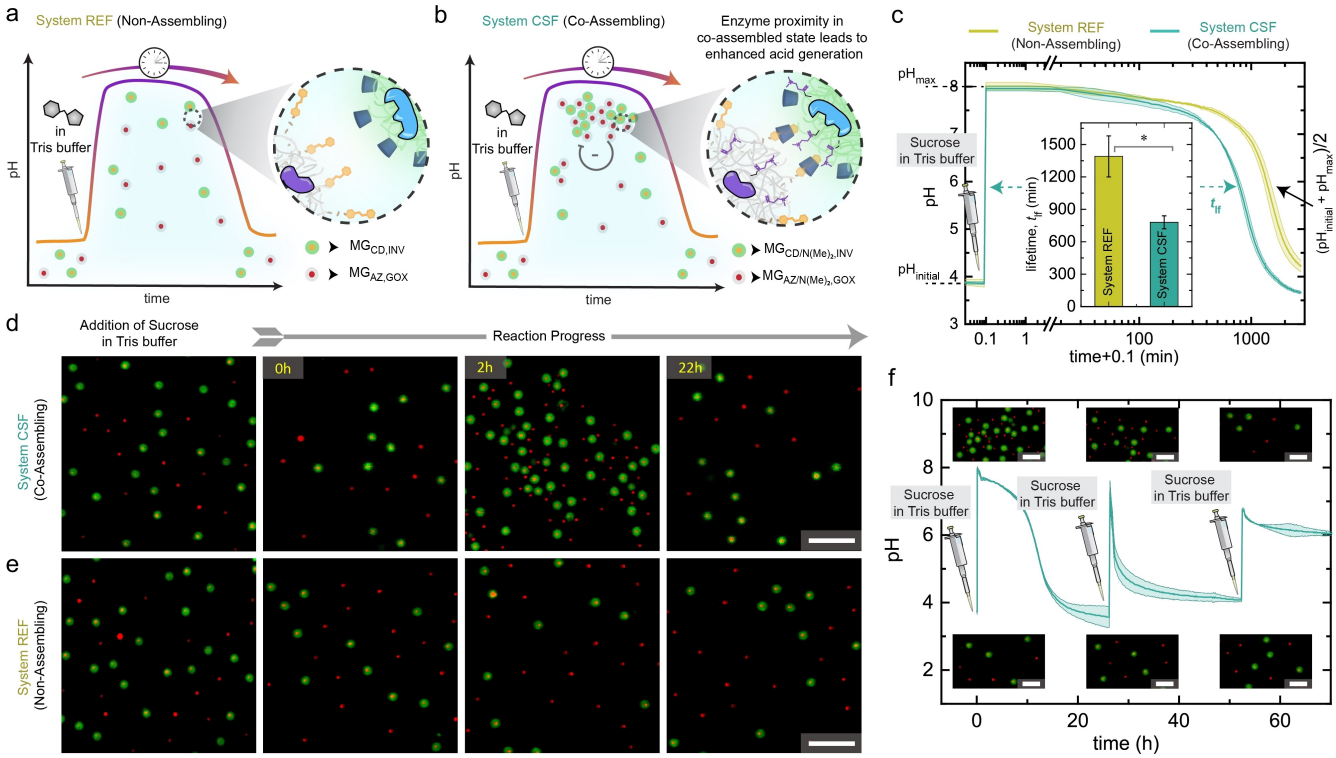

Figure 4. Chemo-structural feedback in transient co-assemblies of MGs. a, b) Schematic representation of two experiments. a) System REF is composed of 1 : 1 mixture of two non-assembling microgels $MG_{CD,INV}$ and $MG_{AZ,GOX}$. b) System CSF is composed of 1 : 1 mixture of two co-assembling microgels $MG_{CD/N(Me)2,INV}$ and $MG_{AZ/N(Me)2,GOX}$. c) pH profiles and lifetimes of both systems. Error bars represent the standard deviation from two independent measurements. * indicate that $p < 0.05$. d, e) ex situ CLSM of System REF (e) and System CSF (d) during the transient state. f) Re-addition of sucrose in tris to 1 : 1 mixture of System CSF leads to dampened response. Conditions: 200 mM sucrose, 1.5 mM CA/NA_3C buffer (pH 3.5), 20 mM tris buffer (pH 8.8), and total concentration of MGs in System REF and System CSF is 0.0064 wt%. All shaded areas represent the standard deviation from two independent measurements. Scale bars: d, e) 5 μm; f) 3 μm.

the pH profiles of REF and CSF can be observed. The pH almost remains constant (or slowly decreases) until 20 minutes due to the low activity of the enzymes (Figure S1), after which CSF takes off and demonstrates a decrease in pH. Moreover, REF is clearly associated with a delayed response which ultimately results in a lifetime ($t_{lf,REF} \approx 1390$ min) ≈ 1.8 times longer than CSF ($t_{lf,CSF} \approx 780$ min).

The lifetime (t_{lf}) is defined as the time that the pH profile takes to decrease to half of the initial pH and the maximum pH. The delay in REF continues until the recorded end point, where the final pH for CSF ($pH_{final} \approx 3.7$) is substantially lower than that for REF ($pH_{final} \approx 4.2$). This effect is even more significant because the activity assays in Figure 3d showed a higher activity of $MG_{AZ,GOX}$ that is used for REF. Concurrently, ex situ CLSM images of REF and CSF confirm that REF remains disassembled over the entire time-period, whereas CSF yields transient co-assembled structures that dissolve autonomously (Figure 4d, e). Collectively, these results conclusively show that the presence of co-assemblies in CSF brings the two enzyme partners close enough to enable enhanced operation of the EC.[15] The consequence is amplified acid generation and the emergence of chemo-structural feedback wherein co-assemblies accelerate their own destruction.

In the interest of a more complete description of such transient systems, we also tested for reactivation using the same fueling solution. Re-addition of sucrose in tris buffer to System CSF leads to successive damping in the pH response (Figure 4f). In a second run, the pH rises to only 7.3 because more equivalents of tris are required for neutralization of previously formed gluconic acid. The resulting pH is neither high enough to trigger co-assemblies nor to access a prolonged plateau. The third injection shows a lower pH feedback to acidic regime, which can stem from waste accumulation.[16]

In summary, we introduced a first rational design approach to reach transient colloidal co-assemblies which accelerate their own destruction by chemo-structural feedback. The approach uses co-assembly of enzyme-loaded MGs to force proximity effects for enhancing an acid-producing EC that accelerates disassembly. Such concepts could be generalized to other chemistries, in particular redox systems, or systems with specific chemical response. Looking out to the future, truly self-regulating systems, in which self-assembling structures take a prominent role in the reaction network by programming their own destruction, are still in their infancy with limited examples. We believe that the concept proposed in this study allows advancements of

transient systems towards autonomously dynamic materials with higher regulatory capacity.

Acknowledgements

We acknowledge funding from the European Union's Horizon 2020 research and innovation program under the Marie Skłodowska-Curie grant agreement no. 812868. We also acknowledge support from the MPI Minerva ARCHES Program. We gratefully acknowledge Dr. S. Ludwanowski for sharing expertise in microgel synthesis. We also thank Dr. I. Maity and Dr. A. Samanta for discussions. A.W. acknowledges support from the Gutenberg Research College. Open Access funding enabled and organized by Projekt DEAL.

Conflict of Interest

The authors declare no conflict of interest.

Data Availability Statement

The data that support the findings of this study are available from the corresponding author upon reasonable request.

Keywords: Chemical Reaction Network · Chemo-Structural Feedback · Colloids · Systems Chemistry · pH-Feedback System

[1] a) D. Philp, J. F. Stoddart, *Angew. Chem. Int. Ed. Engl.* **1996**, *35*, 1154–1196; *Angew. Chem.* **1996**, *108*, 1242–1286; b) G. M. Whitesides, B. Grzybowski, *Science* **2002**, *295*, 2418–2421; c) R. Merindol, A. Walther, *Chem. Soc. Rev.* **2017**, *46*, 5588–5619.

[2] a) M. A. C. Stuart, W. T. S. Huck, J. Genzer, M. Müller, C. Ober, M. Stamm, G. B. Sukhorukov, I. Szleifer, V. V. Tsukruk, M. Urban, F. Winnik, S. Zauscher, I. Luzinov, S. Minko, *Nat. Mater.* **2010**, *9*, 101–113; b) T. Manouras, M. Vamvakaki, *Polym. Chem.* **2017**, *8*, 74–96; c) K. Han, D. Go, D. Hoenders, A. J. C. Kuehne, A. Walther, *ACS Macro Lett.* **2017**, *6*, 310–314; d) K. Han, D. Go, T. Tigges, K. Rahimi, A. J. Kuehne, A. Walther, *Angew. Chem. Int. Ed.* **2017**, *56*, 2176–2182; *Angew. Chem.* **2017**, *129*, 2208–2214; e) M. P. Valignat, O. Theodoly, J. C. Crocker, W. B. Russel, P. M. Chaikin, *Proc. Natl. Acad. Sci. USA* **2005**, *102*, 4225–4229.

[3] L. Heinen, A. Walther, *Soft Matter* **2015**, *11*, 7857–7866.

[4] a) L. Heinen, T. Heuser, A. Steinschulte, A. Walther, *Nano Lett.* **2017**, *17*, 4989–4995; b) T. Heuser, A. K. Steppert, C. M. Lopez, B. Zhu, A. Walther, *Nano Lett.* **2015**, *15*, 2213–2219; c) T. Heuser, E. Weyandt, A. Walther, *Angew. Chem. Int. Ed.* **2015**, *54*, 13258–13262; *Angew. Chem.* **2015**, *127*, 13456–13460; d) X. Fan, A. Walther, *Angew. Chem. Int. Ed.* **2021**, *60*, 11398–11405; *Angew. Chem.* **2021**, *133*, 11499–11506; e) X. Fan, A. Walther, *Angew. Chem. Int. Ed.* **2021**, *60*, 3619–3624; *Angew. Chem.* **2021**, *133*, 3663–3668; f) I. Maity, C. Sharma, F. Lossada, A. Walther, *Angew. Chem. Int. Ed.* **2021**, *60*, 22537–22546; *Angew. Chem.* **2021**, *133*, 22711–22720.

[5] a) S. Maiti, I. Fortunati, C. Ferrante, P. Scrimin, L. J. Prins, *Nat. Chem.* **2016**, *8*, 725–731; b) J. Deng, A. Walther, *Nat. Commun.* **2021**, *12*, 5132; c) S. Dhiman, A. Jain, M. Kumar, S. J. George, *J. Am. Chem. Soc.* **2017**, *139*, 16568–16575; d) J. Deng, A. Walther, *Adv. Mater.* **2020**, *32*, 2002629; e) C. Pezzato, L. J. Prins, *Nat. Commun.* **2015**, *6*, 7790.

[6] a) J. Boekhoven, A. M. Brizard, K. N. K. Kowlgi, G. J. M. Koper, R. Eelkema, J. H. van Esch, *Angew. Chem. Int. Ed.* **2010**, *49*, 4825–4828; *Angew. Chem.* **2010**, *122*, 4935–4938; b) J. Boekhoven, W. E. Hendriksen, G. J. Koper, R. Eelkema, J. H. van Esch, *Science* **2015**, *349*, 1075–1079; c) P. S. Schwarz, M. Tena-Solsona, K. Dai, J. Boekhoven, *Chem. Commun.* **2022**, https://doi.org/10.1039/D1CC06428B; d) J. Heckel, F. Batti, R. T. Mathers, A. Walther, *Soft Matter* **2021**, *17*, 5401–5409; e) J. Heckel, S. Loescher, R. T. Mathers, A. Walther, *Angew. Chem. Int. Ed.* **2021**, *60*, 7117–7125; *Angew. Chem.* **2021**, *133*, 7193–7201; f) M. A. Würbser, P. S. Schwarz, J. Heckel, A. M. Bergmann, A. Walther, J. Boekhoven, *ChemSystemsChem* **2021**, *3*, e2100015; g) L. Heinen, A. Walther, *Sci. Adv.* **2019**, *5*, eaaw0590; h) A. Sorrenti, J. Leira-Iglesias, A. Sato, T. M. Hermans, *Nat. Commun.* **2017**, *8*, 15899; i) J. Deng, A. Walther, *J. Am. Chem. Soc.* **2020**, *142*, 685–689.

[7] I. M. Cheeseman, A. Desai, *Nat. Rev. Mol. Cell Biol.* **2008**, *9*, 33–46.

[8] a) S. Bal, K. Das, S. Ahmed, D. Das, *Angew. Chem. Int. Ed.* **2019**, *58*, 244–247; *Angew. Chem.* **2019**, *131*, 250–253; b) N. Singh, M. P. Conte, R. V. Ulijn, J. F. Miravet, B. Escuder, *Chem. Commun.* **2015**, *51*, 13213–13216; c) B. Sarkhel, A. Chatterjee, D. Das, *J. Am. Chem. Soc.* **2020**, *142*, 4098–4103; d) S. P. Afrose, C. Ghosh, D. Das, *Chem. Sci.* **2021**, *12*, 14674–14685.

[9] a) F. A. Plamper, W. Richtering, *Acc. Chem. Res.* **2017**, *50*, 131–140; b) D. Suzuki, T. Sakai, R. Yoshida, *Angew. Chem. Int. Ed.* **2008**, *47*, 917–920; *Angew. Chem.* **2008**, *120*, 931–934; c) D. Suzuki, H. Taniguchi, R. Yoshida, *J. Am. Chem. Soc.* **2009**, *131*, 12058–12059.

[10] F. Scheffold, *Nat. Commun.* **2020**, *11*, 4315.

[11] a) A. Harada, R. Kobayashi, Y. Takashima, A. Hashidzume, H. Yamaguchi, *Nat. Chem.* **2011**, *3*, 34–37; b) J. Moratz, A. Samanta, J. Voskuhl, S. K. Mohan Nalluri, B. J. Ravoo, *Chem. Eur. J.* **2015**, *21*, 3271–3277.

[12] Q.-L. Li, W.-X. Gu, H. Gao, Y.-W. Yang, *Chem. Commun.* **2014**, *50*, 13201–13215.

[13] E. Daly, B. R. Saunders, *Phys. Chem. Chem. Phys.* **2000**, *2*, 3187–3193.

[14] F. Jia, B. Narasimhan, S. Mallapragada, *Biotechnol. Bioeng.* **2014**, *111*, 209–222.

[15] M. Castellana, M. Z. Wilson, Y. Xu, P. Joshi, I. M. Cristea, J. D. Rabinowitz, Z. Gitai, N. S. Wingreen, *Nat. Biotechnol.* **2014**, *32*, 1011–1018.

[16] C. M. Wong, K. H. Wong, X. D. Chen, *Appl. Microbiol. Biotechnol.* **2008**, *78*, 927–938.

Manuscript received: January 28, 2022
Accepted manuscript online: March 2, 2022
Version of record online: March 14, 2022